The Feasibility of Assessing Perfusion of the Bone Using Quantitative ICG Fluorescence Imaging

Danielle Boldewijn, MD[1] Marlies Michi, MD[2] Jan Maerten Smit, MD[1] Hanneke Joosten, MD, PhD[3] Daniel de Bruin, MSc, PhD[4,5] Richard van den Elzen, MSc[4] Caroline Driessen, MD, PhD[1]

[1] Department of Plastic Surgery, Amsterdam University Medical Center, HV Amsterdam, The Netherlands
[2] Department of Plastic Surgery, University Medical Center Groningen, Hanzeplein 1, The Netherlands
[3] Department of Surgery, Amsterdam University Medical Center, Amsterdam, The Netherlands
[4] Department of Biomedical Engineering and Physics, Amsterdam University Medical Center, Amsterdam, The Netherlands
[5] Department of Urology, Amsterdam University Medical Center, Amsterdam, The Netherlands

Address for correspondence Caroline Driessen, MD, PhD, Department of Plastic Surgery, Amsterdam University Medical Center;, location VUmc, De Boelelaan 1117, 1081 HV Amsterdam, The Netherlands (e-mail: c.driessen@amsterdamumc.nl).

J Reconstr Microsurg Open 2024;9:e113–e120.

Abstract

Background Near-infrared fluorescence (NIRF) imaging using indocyanine green (ICG) allows perfusion to be visualized and objective perfusion parameters can be provided after additional measurements. Therefore, it has great potential in predicting adequate tissue perfusion. However, regarding bone tissue, evidence of the feasibility and usefulness of NIRF imaging using ICG is very limited.

Methods A prospective monocentric pilot study was carried out at a tertiary hospital in the Netherlands. Patients undergoing autologous breast reconstruction from August 2021 to August 2022 were included. During surgery, ICG (0.1 mg/kg) was injected intravenously and a fluorescent angiogram of 4 minutes was made directly after injection. Post hoc time-intensity curves were generated for a 5-mm region of interest (ROI) positioned on the cross-sectional lateral surface of the rib. The first moment of increase of intensity was defined as t0. Fluorescent parameters included ingress and egress of ICG.

Results Nine patients and 11 ribs were included for further analysis. Time-intensity curves were generated for endosteal measurement in 10 ribs. Three of the curves showed a steep and well-defined ingress and egress. In all other patients, the curves showed a much more flattened ingress and egress. Periosteal measurement was performed in nine ribs. No adverse events related to the ICG injection were observed intraoperatively.

Conclusion This feasibility study suggests that quantitative NIRF imaging using ICG can provide objective parameters of endosteal rib perfusion. Larger prospective series are needed to investigate the value of NIRF imaging using ICG to assess bone perfusion intraoperatively and to establish cutoff values for adequate bone perfusion.

Keywords
- fluorescence imaging
- ICG
- bone perfusion

received
June 11, 2024
accepted after revision
July 23, 2024
accepted manuscript online
August 27, 2024

DOI https://doi.org/10.1055/a-2404-1848.
ISSN 2377-0813.

Thieme Medical Publishers, Inc., 333 Seventh Avenue, 18th Floor, New York, NY 10001, USA

Adequate bone perfusion is key for successful surgery. It is important for healing and consolidation, particularly in cases of traumatic crush injuries or when subsequent radiotherapy is necessary.

Over the years, several techniques have been developed to support surgeons in assessing adequate tissue perfusion. One of them is near-infrared fluorescence (NIRF) imaging, using indocyanine green (ICG). ICG is a water-soluble fluorescence dye and when administered intravenously, it binds to 98% plasma proteins and is therefore an ideal tracer to measure perfusion. ICG has a half-life of 3 to 4 minutes, and it is cleared exponentially by the liver with a clearance rate of approximately 20% per minute.[1,2] ICG is considered very safe for patients, since anaphylactic reactions are rare with an incidence of 0.05%.[3] The light required for the excitation of ICG is generated by a light source that is directly attached to a digital video camera with a specific filter. This light source emits light between 750 and 800 nm, which is near the infrared range and excites ICG, which can be viewed around the maximum peak of 832 nm.[1,4] With NIRF imaging using ICG, the absorption of ICG can be recorded real time during surgery and allows perfusion assessment. Owing to its encouraging results, NIRF imaging has grown in popularity across a variety of surgical specialties, including reconstructive surgery.[5–8]

Visualizing bone perfusion is challenging. It would be of great interest to evaluate the application of NIRF imaging using ICG for osseous tissue. For example, it could be highly valuable when assessing vascularized bone flaps, especially when they need to be osteotomized for head and neck reconstructions or extremity reconstructions where adequate perfusion is key for consolidation. Moreover, it could improve the early debridement of necrotic bone in extended trauma cases, may improve the identification of sequesters, and could be useful in the removal of tissue affected by osteoradionecrosis.[9–12]

To provide objective perfusion parameters and fluorescence intensity curves of bone tissue, this study investigated the perfusion of the human rib with NIRF imaging using ICG. The rib is easily accessible when anastomosing a free flap in autologous breast reconstruction. Bones have a bipartite blood supply consisting of endosteal and periosteal networks, which are connected through small capillaries.[13–15] The endosteal blood supply is provided by the nutrient artery, which is a branch of the posterior intercostal artery. The nutrient artery enters the medullary canal of the rib just beyond the tubercle, which is located posteriorly.[16,17] The internal mammary vessels, which arise from the subclavian vessels, branch into the inferior intercostal vessels (►**Fig. 1**). The periosteal circulation of the ribs is based on dual blood supply provided by the inferior intercostal vessels and the superior supracostal vessels. These vessels have interconnecting arterioles covering the whole surface of the rib.[18] It is thought that the nutrient artery is necessary for survival of the rib.[19] Conversely, studies have shown that the viability of the rib is sustained on periosteal blood supply alone.[20–24]

Objective fluorescence parameters of bone perfusion are sparse.[25] There are solely five studies in which outcomes are reported, including relative perfusion and absolute

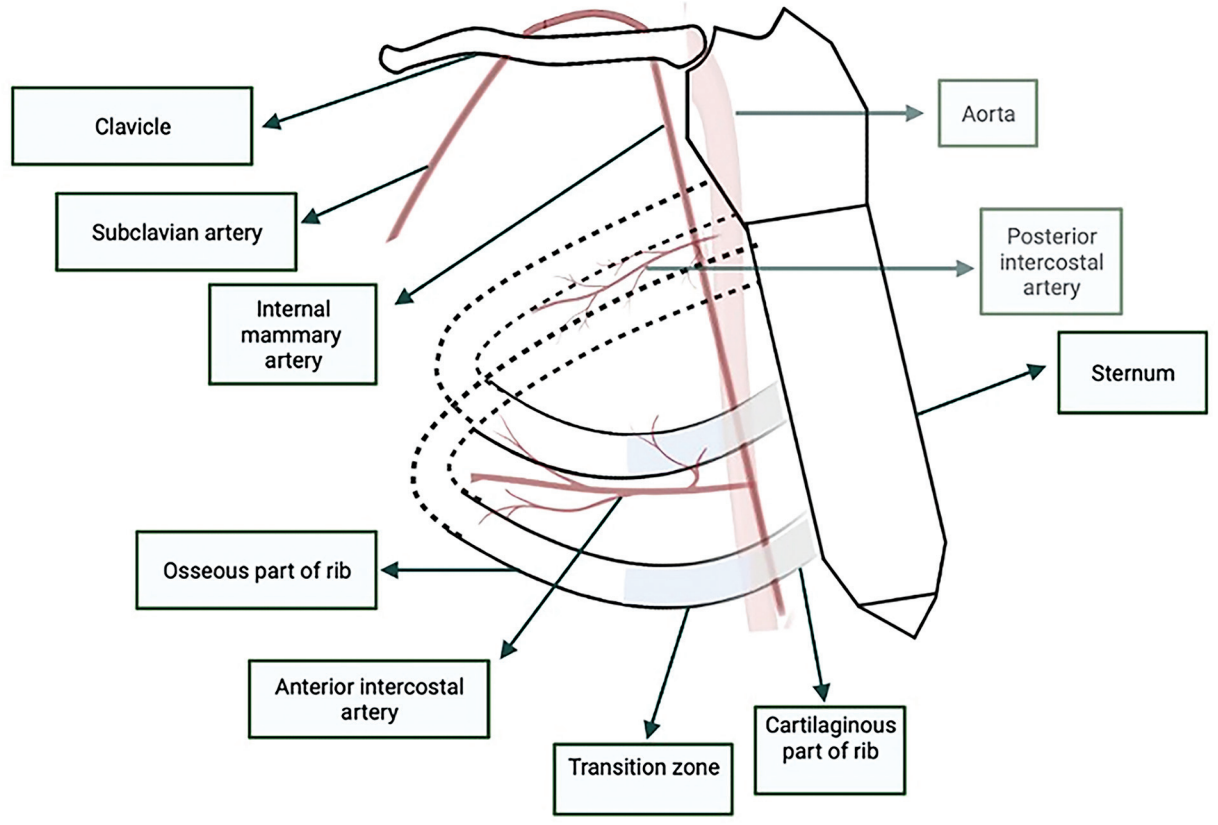

Fig. 1 Diagram showing the anatomy of the rib, including the internal mammary artery, also known as the internal thoracic artery.

perfusion.[26–30] One study reported the relative perfusion parameter defined as the fluorescence intensity at a region of interest (ROI) divided by the background fluorescence.[26] Others defined absolute perfusion parameters as maximum fluorescence intensity over time.[27–29] Some of these outcomes are investigated in human studies and others in animal studies. Quantitative interpretation of fluorescence imaging has as main limitation that it is subject to inter-user interpretation. Qualitative parameters may overcome this limitation. There is no consensus on a standardized manner or which parameters should be used to assess bone perfusion. However, dynamic perfusion parameters such a fluorescence intensity curves seemed effective for evaluating perfusion.[31] To date, these dynamic parameters have not yet been studied for bone perfusion in humans.

The aim of this pilot study is to assess the feasibility of fluorescence imaging of the rib, in order to provide objective perfusion parameters of bone.

Materials and Methods

Participants

This feasibility study was carried out at a tertiary hospital in the Netherlands. A total of 13 patients undergoing primary or secondary autologous breast reconstruction from August 2021 to August 2022 were included in this study before surgery. The exclusion criteria were the following: younger than 18 years, hyperthyroidism, autonomic thyroid adenoma, epilepsy, renal failure with estimated glomerular filtration rate (eGFR) < 60, severe liver failure, and patients who are allergic to ICG, iodine, or shellfish. All the data were collected in Castor (CDMS version 2022.3). The study was approved by the Ethics Committee of Amsterdam University Medical Center (2021.0142). All patients provided written informed consent. Preoperative data recorded included patient's age, height, weight, body mass index (BMI), medical history, history of smoking, and family history. Intraoperative recorded data included vital parameters such as blood pressure, heart rate, saturation, and use of vasopressors during administration of ICG.

Surgery and Fluorescence Imaging

In all patients undergoing autologous breast reconstruction, the medial portion of approximately 2 cm of the second or third rib was removed to perform arterial and venous anastomoses of the flap to the internal mammary vessels (►**Fig. 2**). After revascularization, the rib was exposed, and a camera was positioned at approximately 30 cm above the rib and pointed transverse to the rib with the periosteum visible. A dose of 0.1 mg/kg of ICG (Verdye 25 mg) was injected intravenously. Subsequently, fluorescent intensity was captured by the Tivato 700 microscope (Carl Zeiss Meditec AG, 2019, Jena Germany) for 4 minutes (►**Fig. 3**). During the fluorescent assessment, ambient light was dimmed.

Quantification of the Fluorescent Signal

Postoperatively, video images were quantified using a tailor-made software written in the Python v3.8 programming language (Python Software Foundation, https://www.python.org/). For endosteal measurement, the ROI of 5 mm was positioned on the cross-sectional, lateral surface of the rib by the first author (D.F.B.). The ROI was also positioned by a second observer (M.M.) to analyze interobserver reliability. Also, an ROI was positioned on the anastomosed blood vessels where blood perfusion is considered to be optimal and, if feasible, also on a region of bone with intact periosteum for periosteal measurement. For all ROIs, the software generated time-intensity curves of the measured intensity in arbitrary units (a.u.). From these curves, perfusion parameters were extracted, which are illustrated in detail in ►**Fig. 4**. Ingress was defined as the increase in fluorescence intensity per second, from baseline to

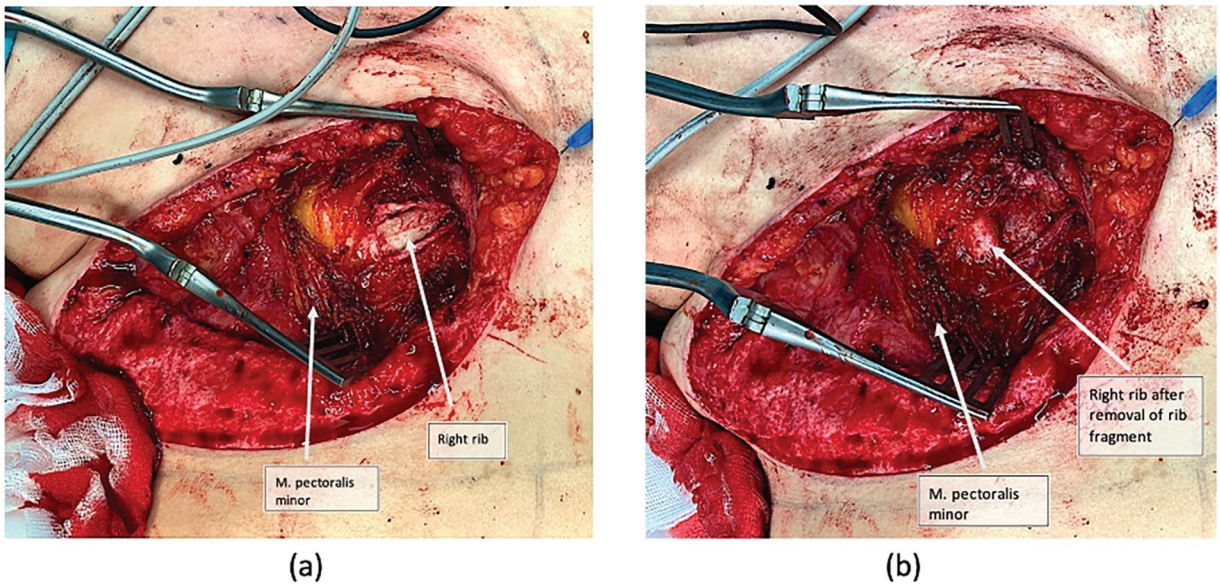

Fig. 2 Intraoperative photograph throughout autologous breast reconstruction of the right breast, showing the visual (**a**) before and (**b**) after removal of the rib fragment in which the lateral cross-sectional surface becomes visible. M., muscle.

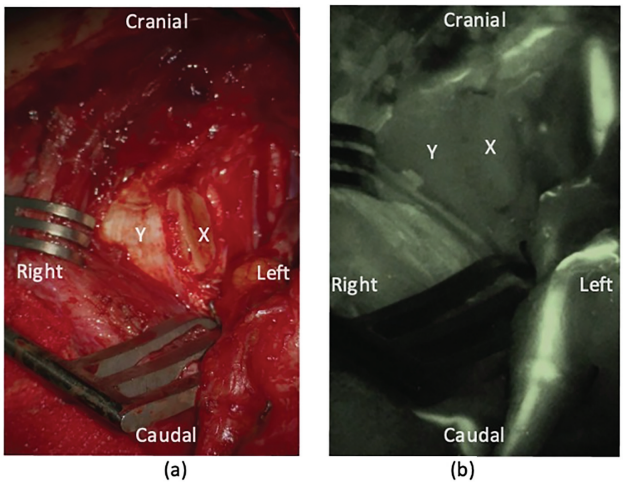

Fig. 3 Near-infrared fluorescence (NIRF) imaging using indocyanine green intraoperative in a patient showing the (**a**) visual and (**b**) NIRF fluorescence in the rib (X: endosteal region of interest; Y: periosteal region of interest).

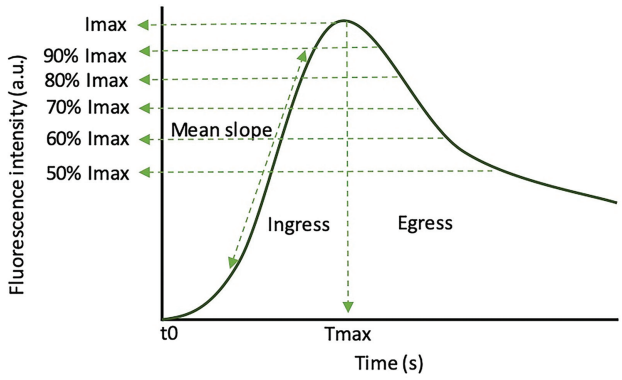

Fig. 4 Time-intensity curve with extracted perfusion parameters. Imax, maximum intensity. Tmax is the time at which the intensity is at its maximum.

maximum fluorescence intensity (Imax). Relative perfusion was defined as the maximum fluorescence intensity of ROI at anastomosed blood vessel divided by maximum fluorescence intensity at ROI. Mean slope was calculated as Δintensity/Δtime. Normalized maximum slope is calculated by dividing the mean slope at the steepest point of the ingress curve by the total slope of the ingress curve ((Δintensity/Δtime)/Imax – I0). Egress was defined as the decrease in ICG fluorescence intensity per second, from Imax until last measurement. The starting time of the curves (t0) was defined as the first moment of increase in intensity compared to baseline.

Patients with videos of blurry image were excluded.

The median values of the measured intensities in the ROI for each video were calculated. Statistical analysis was performed using IBM SPSS 26.0 (IBM, Armonk, NY, United States). Normality was assessed using the Shapiro–Wilk test and data were presented as median with minimum and maximum values. For continuous variables, the Wilcoxon signed-rank test was used. Interobserver reliability was calculated using the intraclass correlation coefficient with an absolute agreement definition.

Table 1 Patient characteristics

Characteristics	Number of patients ($n = 9$)
Mean age, y (SD)	53.1 (4.6)
Mean BMI, kg/m^2 (SD)	28.2 (3.1)
Diabetes mellitus	0
Hypertension	2
Hypercholesterolemia	0
Active smoking	0
Type of autologous breast reconstruction	
DIEP flap	7
SGAP flap	1
Omental flap	1

Abbreviations: BMI, body mass index; DIEP, deep inferior epigastric perforator; SD, standard deviation; SGAP, superior gluteal artery perforator.

Results

Patient Characteristics and Outcomes

Thirteen patients were included, of which 4 patients were excluded. Two were excluded due to videos of blurry image and two were excluded because a different surgical technique was used to remove the rib fragment.

As a result, 9 patients were included and 11 ribs were analyzed. From these patients, there were seven deep inferior epigastric artery perforator (DIEP) reconstructions including two bilateral DIEP reconstructions, one superior gluteal artery perforator (SGAP) reconstruction, and one omental flap reconstruction. The video of patient 5 was only suitable for periosteal measurement and the videos of patient 2 and 5 were suitable only for endosteal measurement.

Patient characteristics are displayed in ►**Table 1**. No adverse events related to ICG injection were observed intraoperatively. Intraoperative vital parameters and patient specifications are shown in ►**Table 2**.

Time-Intensity Curves

Time-intensity curves for endosteal measurement were generated for 10 ribs and are shown in ►**Fig. 5**. There are two distinct patterns in the ICG ingress phase. First, a steep slope reached within 10 seconds after t0 was observed in patients 2, 6, and 7. In other patients, ingress was less steep and turned into a flattened slope.

Regarding the ICG egress phase, three distinct patterns were observed. Three curves showed a steep slope, which turned quickly into a flattened slope (patients 2, 6, and 7). In four curves, egress was clearly prolonged (patients 1b, 3, 4, and 9b). In the three remaining curves (patients 1a, 8, and 9a), egress had not begun within the 240-second measurement period.

To summarize, patients 2, 6, and 7 had steep and well-defined ingress and egress. In all other patients, the curves showed a much more flattened ingress and egress.

Table 2 Patient specifications

	Characteristics			Vital parameters		
	Radiation therapy	Smoking	Cardiovascular comorbidity	Blood pressure (mm Hg)	Heart rate (beats/min)	Saturation (%)
Patient 1[a]	No	Former	No	95/55	57	100
Patient 2	No	No	No	113/59	65	100
Patient 3	No	No	No	100/60	80	98
Patient 4	No	No	HT	118/63	60	99
Patient 5	No	No	No	93/50	81	100
Patient 6	Yes	Former	No	115/60	65	98
Patient 7	No	No	No	96/53	46	100
Patient 8	No	Former	No	110/63	53	97
Patient 9[a]	No	No	HT	93/50	54	98

Abbreviations: HT, hypertension.
Note: Vital parameters were collected at the time of injecting of indocyanine green. The patient is former smoker who quit smoking more than 1 month ago.
[a]The patient is undergoing a bilateral deep inferior epigastric artery perforator and will continue as patient "a" and patient "b."

Quantitative Analysis

The outcomes of quantitative analysis on the time-intensity curves of the endosteal and periosteal ROI are shown in ►**Table 3**. The median maximum intensity was 94.6 a.u. in the endosteal ROI as compared to 89.1 a.u. in the periosteal ROI ($p = 0.889$). The median mean slope and the median normalized maximum slope were slightly higher in the periosteal ROI (0.8 vs. 1.2, $p > 0.726$; 0.1 vs. 1.5, $p > 0.161$. Among the observers (D.F.B. and M.M.), there was an excellent agreement about the positioning of the ROI with an intraclass correlation coefficient of 94.3%.

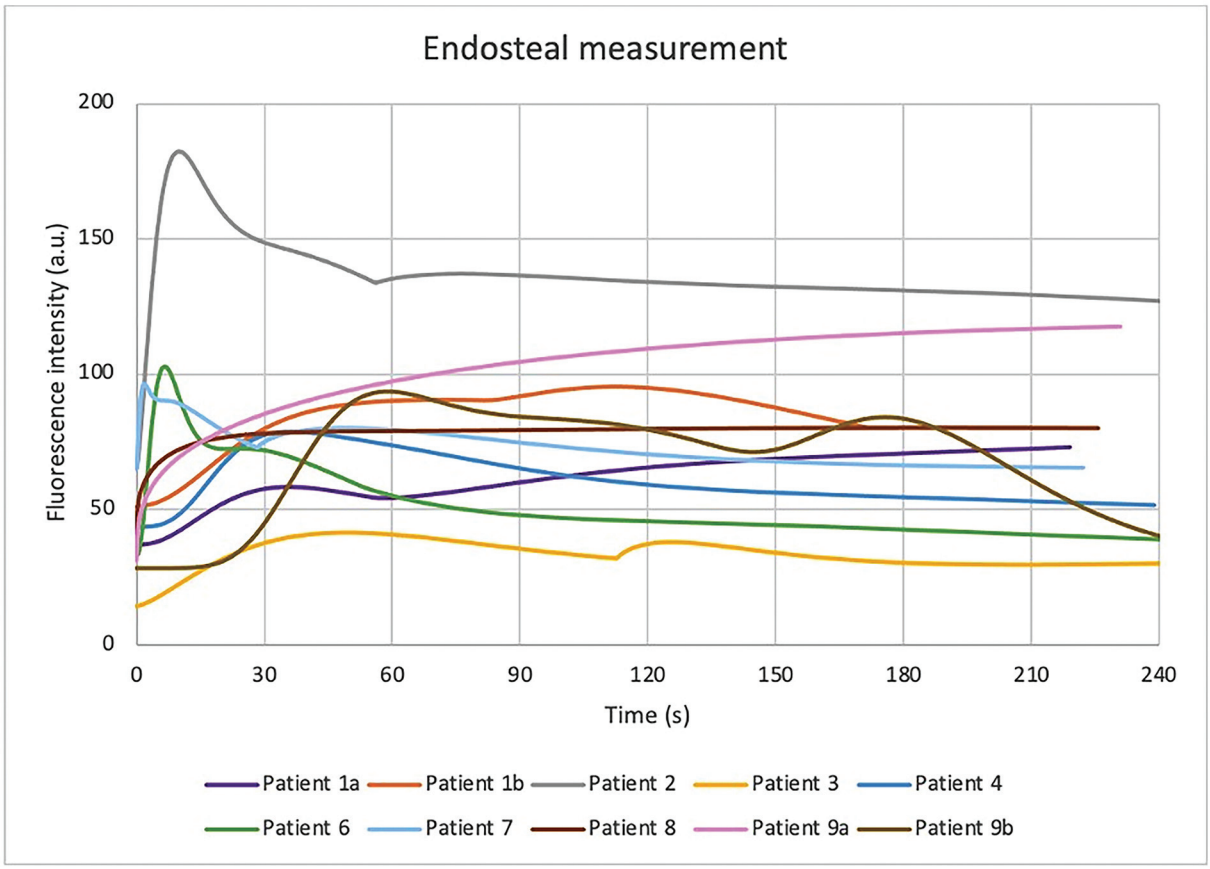

Fig. 5 Time-intensity curves of endosteal measurement of the rib.

Table 3 Quantitative assessment NIRF imaging

Parameter of ingress	Endosteal	Periosteal
	Median (minimum–maximum)	Median (minimum–maximum)
Imax (a.u.)[a]	94.6 (41.5–182.4)	89.1 (44.4–110.71)
Time from t0 to Imax (s)	54.4 (1.8–230.8)	59.4 (1.0–224.3)
Relative perfusion (%)	2.5 (1.2–4.7)	3.1 (1.7–4.6)
Mean slope	0.8 (0.2–17.4)	1.2 (0.2–63.9)
Normalized maximum slope	0.1 (0.0–3.9)	1.5 (0.1–3.1)
Parameter of egress		
	Number of ribs ($n = 10$)	Number of ribs ($n = 9$ ribs)
90% Imax	7	6
80% Imax	6	6
70% Imax	5	5
60% Imax	2	3
50% Imax	2	1

Abbreviations: Imax, maximum intensity; NIRF, near-infrared fluorescence.
[a]Median maximum intensity at the blood vessel was 224.0 a.u. (163.6–274.7)

Discussion

In this pilot study, we were able to quantify perfusion of the human rib with NIRF imaging using ICG. This was shown with measurements in two different ROIs: endosteal and periosteal. According to several anatomical studies, the osseous blood supply is bipartite and depends on the endosteal and periosteal blood supply.[14,15,32] In the 11 measurements in the study, the endosteal and periosteal parameters show much agreement with no statistically significant differences. Numerous clinical applications in soft-tissue surgery have been studied for NIRF imaging using ICG.[33–36] There are only five previous studies that report on objective NIRF outcomes for bone perfusion.[26–30] It is notoriously difficult to assess the viability of bone based on clinical signs, but accurate debridement of nonviable bone is crucial. The relative perfusions of 2.5% (endosteal) and 3.1% (periosteal) confirm that perfusion of the rib is quite low as compared to the perfusion at the level of the anastomosed blood vessels.

Thorough debridement without wasting additional bone is extremely important to accomplish optimal bone healing, bone reconstruction, and cure. Fluorescence imaging may play a role in debridement after trauma injury of the extremities, long-lasting infectious disease of the tibia, femur, and humerus, or osteoradionecrosis after breast (rib), rectum (sacrum), and oropharyngeal tumors ((neo-)mandible).[12] Moreover, it may have an interesting role in osseous reconstructions such as free vascularized fibula grafts, especially when multiple osteotomies are necessary.[28] The scientific evidence for using NIRF to visualize bone perfusion is sparse.[25] Yoshimatsu et al evaluated bone perfusion in cadaveric femoral medial condyle.[37] They compared the penetration depth of methylene blue with NIRF imaging using ICG. Following injection of methylene blue and ICG into the descending genicular artery, the cancellous area was visible with NIRF imaging due to tiny perforators that penetrated the periosteum in contrary to the blue dye that was solely visible in the periosteum. Nguyen et al was able to demonstrate that endosteal perfusion and viability of vascularized bone flaps can be assessed with NIRF imaging using ICG.[26] This was shown in osteomyocutaneous forelimb flaps and fibula flaps of female Yorkshire pigs. They compared a devascularized bone flap, in which the pedicle had been ligated, to a vascularized bone flap using NIRF imaging. The vascularized flap showed NIRF perfusion at the osteotomy site, whereas the devascularized flap showed a lack of fluorescence. Gitajn et al demonstrated in porcine models that bone perfusion can be measured quantitatively from endosteal and periosteal sources using NIRF imaging with ICG.[29] Fichter et al[28] and Gitajn et al[29] defined absolute perfusion values as maximum fluorescence in number of units at a specific moment in time and extracted time-intensity curves, whereas Valerio et al[27] focused on maximum fluorescence at a single unspecified time point without extracting time-intensity curves. Gitajn et al[29] and Elliot et al[30] studied ICG fluorescence curves of ROIs in bone under various damage situations, and a new kinetic model was created and used. The underlying idea behind this model is that the bone ICG fluorescence curve reflects both "early" and "late" bone perfusion and once again represents the bone's bipartite blood supply network. Gitajn et al demonstrated that when the periosteal blood supply was disrupted by stripping soft tissue from the bone, maximum fluorescence intensity decreased by 50% and time to reach maximum fluorescence intensity increased.[29] This suggests that "late" bone perfusion is connected to endosteal blood supply, while "early" bone perfusion and periosteal blood supply are connected to one another.

Absolute and relative perfusion values do not offer insight into how intensity changes over time. Additionally, absolute perfusion is dependent on the measured fluorescence intensity and hence prone to several influencing factors including

camera distance and camera angle.[31,38] Among the endosteal and periosteal ROIs that we obtained, the extracted time-intensity curves demonstrated several patterns of ICG ingress and egress. In the endosteal view, a steep ingress was recognized with a steep egress in three ribs and the majority of the observed curves demonstrated a prolonged egress. In others, ingress is less steep and egress is flat or does not start at all. For several subjects in this study, the 4-minute measurement period was insufficient to observe the initiation of venous outflow. In other studies, these flat curves with slow ingress and slow or absent egress represent bad perfusion with suboptimal inflow and outflow.[39–42]

Quantitative perfusion analysis in studies focusing on the esophagus, ileum, and colon tissue often shows a good inflow and a well-defined egress in case of good tissue perfusion. We find these curves in three of the ribs that we studied. The majority of the ribs, however, showed a slow ingress and a flat or absent egress. This may be explained by a more medial ostectomy, at the level where the rib is most cartilaginous. Cartilage is notoriously badly perfused. As a result, the intensity curves in cartilaginous bone tissue may be different from the curves that are often found in well-vascularized tissue during gastrointestinal surgery.[39–42] The well-defined curves with a steep ingress and well-defined egress may match the patients with a more spongy rib or patients in whom the ostectomy of the rib was extended laterally. However, this cannot be confirmed in hindsight. Other factors that may influence the shape of the curve are iatrogenic damage of the periosteum during surgical dissection, environmental influences such as light, heat, and manipulation leading to vasoconstriction, or blood dripping onto the ROI.

Some limitations were observed in this study. The measurement of maximum fluorescence intensity is influenced by multiple environmental factors, such as camera distance, camera angle, ambient light, blood pressure, and use of intraoperative medication. This may also explain why the fluorescence intensity curves do not start from zero. Due to the small sample size of this study, it was not possible to establish the effect of all these parameters on fluorescence intensity and its dynamics. Moreover, it was hard to position the camera adequately to capture an endosteal and periosteal ROI in one view. This resulted in two ribs in which only one ROI was visible. Despite these limitations, this study provides insight into the possibility of quantification of bone perfusion, showing promising results. This study demonstrated that it is challenging, but feasible to use NIRF imaging to study the rib. This is a step toward the use of NIRF imaging with ICG to provide surgeons with quantitative parameters for assessing bone perfusion.

Based on our first experience of quantifying rib perfusion, we recommend the following: keep all external parameters stable, prolong the video for more than 5 minutes, and ensure there is an ROI with sufficient perfusion available in the field of view. A larger cohort is needed to investigate the value of the inflow parameters in the assessment of bone perfusion to correlate divergent parameters to patient-specific factors and for the prediction of clinical outcomes. To minimize movement artifacts due to breathing, bone perfusion in, for example, a healthy fibula graft should be measured. Taken this into account, it should be possible to establish reliable cutoff values for normal bone perfusion. Therefore, more research is needed to investigate the possibilities of using NIRF imaging with ICG to assess bone perfusion intraoperatively. Cutoff values are needed to guide a surgeon in the debridement of affected bone or reconstructive surgery with vascularized bone.

Conclusion

This study demonstrated the feasibility of quantification of perfusion in human ribs using NIRF imaging with ICG. The result of our study suggests that NIRF imaging using ICG can provide surgeons with objective parameters for assessing bone perfusion. However, implementing our NIRF imaging results of bone perfusion into surgery remains a challenge.

Conflict of Interest
None declared.

References

1 Mordon S, Devoisselle JM, Soulie-Begu S, Desmettre T. Indocyanine green: physicochemical factors affecting its fluorescence in vivo. Microvasc Res 1998;55(02):146–152
2 Muckle TJ. Plasma proteins binding of indocyanine green. Biochem Med 1976;15(01):17–21
3 Hope-Ross M, Yannuzzi LA, Gragoudas ES, et al. Adverse reactions due to indocyanine green. Ophthalmology 1994;101(03):529–533
4 Braun JD, Trinidad-Hernandez M, Perry D, Armstrong DG, Mills JL Sr. Early quantitative evaluation of indocyanine green angiography in patients with critical limb ischemia. J Vasc Surg 2013;57(05):1213–1218
5 Wilke BK, Schultz DS, Huayllani MT, et al. Intraoperative indocyanine green fluorescence angiography is sensitive for predicting postoperative wound complications in soft-tissue sarcoma surgery. J Am Acad Orthop Surg 2021;29(10):433–438
6 Patel KM, Bhanot P, Franklin B, Albino F, Nahabedian MY. Use of intraoperative indocyanin-green angiography to minimize wound healing complications in abdominal wall reconstruction. J Plast Surg Hand Surg 2013;47(06):476–480
7 Phillips BT, Lanier ST, Conkling N, et al. Intraoperative perfusion techniques can accurately predict mastectomy skin flap necrosis in breast reconstruction: results of a prospective trial. Plast Reconstr Surg 2012;129(05):778e–788e
8 Momeni A, Sheckter C. Intraoperative laser-assisted indocyanine green imaging can reduce the rate of fat necrosis in microsurgical breast reconstruction. Plast Reconstr Surg 2020;145(03):507e–513e
9 Pruimboom T, Schols RM, Qiu SS, van der Hulst RRWJ. Potential of near-infrared fluorescence image-guided debridement in trauma surgery. Case Reports Plast Surg Hand Surg 2018;5(01):41–44
10 Koshimune S, Shinaoka A, Ota T, Onoda S, Kimata Y. Laser-assisted indocyanine green angiography aids in the reconstruction of Gustilo grade IIIB open lower-limb fractures. J Reconstr Microsurg 2017;33(02):143–150
11 Amaechi BT, Owosho AA, Fried D. Fluorescence and near-infrared light transillumination. Dent Clin North Am 2018;62(03):435–452
12 Green JM III, Sabino J, Fleming M, Valerio I. Intraoperative fluorescence angiography: a review of applications and outcomes in war-related trauma. Mil Med 2015;180(3, Suppl):37–43

13 Oni OO, Stafford H, Gregg PJ. An experimental study of the patterns of periosteal and endosteal damage in tibial shaft fractures using a rabbit trauma model. J Orthop Trauma 1989;3 (02):142–147
14 Wei FC, Chen HC, Chuang CC, Noordhoff MS. Fibular osteoseptocutaneous flap: anatomic study and clinical application. Plast Reconstr Surg 1986;78(02):191–200
15 Menck J, Sander A. [Periosteal and endosteal blood supply of the human fibula and its clinical importance]. Acta Anat (Basel) 1992; 145(04):400–405
16 Daniel RK. Free rib transfer by microvascular anastomoses. Plast Reconstr Surg 1977;59(05):737–738
17 Couly G, Vaillant JM, Cernea P, Ginisty D, Evans J. The blood supply of the human rib and the use of free rib grafts with microanastomosis between the posterior intercostal and facial arteries in mandibular reconstruction. Int J Microsurg 1979;1 (01):22–26
18 Thoma A, Heddle S, Archibald S, Young JE. The free vascularized anterior rib graft. Plast Reconstr Surg 1988;82(02):291–298
19 Ostrup LT, Fredrickson JM. Distant transfer of a free, living bone graft by microvascular anastomoses. An experimental study. Plast Reconstr Surg 1974;54(03):274–285
20 McKee DM. Microvascular bone transplatation. Clin Plast Surg 1978;5(02):283–292
21 Ariyan S, Finseth FJ. The anterior chest approach for obtaining free osteocutaneous rib grafts. Plast Reconstr Surg 1978;62(05): 676–685
22 Song R, Lu C, Song Y, Liu J. Repair of large mandibular defects with vascularized rib grafts. Clin Plast Surg 1982;9(01):73–78
23 Ariyan S. The viability of rib grafts transplanted with the periosteal blood supply. Plast Reconstr Surg 1980;65(02):140–151
24 Strauch B, Bloomberg AE, Lewin ML. An experimental approach to mandibular replacement: island vascular composite rib grafts. Br J Plast Surg 1971;24(04):334–341
25 Michi M, Madu M, Winters HAH, de Bruin DM, van der Vorst JR, Driessen C. Near-infrared fluorescence with indocyanine green to assess bone perfusion: a systematic review. Life (Basel) 2022;12 (02):154
26 Nguyen JT, Ashitate Y, Buchanan IA, et al. Bone flap perfusion assessment using near-infrared fluorescence imaging. J Surg Res 2012;178(02):e43–e50
27 Valerio I, Green JM III, Sacks JM, Thomas S, Sabino J, Acarturk TO. Vascularized osseous flaps and assessing their bipartate perfusion pattern via intraoperative fluorescence angiography. J Reconstr Microsurg 2015;31(01):45–53
28 Fichter AM, Ritschl LM, Georg R, et al. Effect of segment length and number of osteotomy sites on cancellous bone perfusion in free fibula flaps. J Reconstr Microsurg 2019;35(02):108–116
29 Gitajn IL, Elliott JT, Gunn JR, et al. Evaluation of bone perfusion during open orthopedic surgery using quantitative dynamic contrast-enhanced fluorescence imaging. Biomed Opt Express 2020;11(11):6458–6469
30 Elliott JT, Jiang S, Pogue BW, Gitajn IL. Bone-specific kinetic model to quantify periosteal and endosteal blood flow using indocyanine green in fluorescence guided orthopedic surgery. J Biophotonics 2019;12(08):e201800427
31 Goncalves LN, van den Hoven P, van Schaik J, et al. Perfusion parameters in near-infrared fluorescence imaging with indocyanine green: a systematic review of the literature. Life (Basel) 2021;11(05):433
32 Taylor GI, Miller GD, Ham FJ. The free vascularized bone graft. A clinical extension of microvascular techniques. Plast Reconstr Surg 1975;55(05):533–544
33 Lee BT, Hutteman M, Gioux S, et al. The FLARE intraoperative near-infrared fluorescence imaging system: a first-in-human clinical trial in perforator flap breast reconstruction. Plast Reconstr Surg 2010;126(05):1472–1481
34 Mieog JS, Troyan SL, Hutteman M, et al. Toward optimization of imaging system and lymphatic tracer for near-infrared fluorescent sentinel lymph node mapping in breast cancer. Ann Surg Oncol 2011;18(09):2483–2491
35 Gioux S, Mazhar A, Lee BT, et al. First-in-human pilot study of a spatial frequency domain oxygenation imaging system. J Biomed Opt 2011;16(08):086015
36 Liu DZ, Mathes DW, Zenn MR, Neligan PC. The application of indocyanine green fluorescence angiography in plastic surgery. J Reconstr Microsurg 2011;27(06):355–364
37 Yoshimatsu H, Steinbacher J, Meng S, et al. Feasibility of bone perfusion evaluation in cadavers using indocyanine green fluorescence angiography. Plast Reconstr Surg Glob Open 2017;5(11): e1570
38 Lütken CD, Achiam MP, Svendsen MB, Boni L, Nerup N. Optimizing quantitative fluorescence angiography for visceral perfusion assessment. Surg Endosc 2020;34(12):5223–5233
39 Lütken CD, Achiam MP, Osterkamp J, Svendsen MB, Nerup N. Quantification of fluorescence angiography: toward a reliable intraoperative assessment of tissue perfusion—a narrative review. Langenbecks Arch Surg 2021;406(02):251–259
40 Gosvig K, Jensen SS, Qvist N, et al. Quantification of ICG fluorescence for the evaluation of intestinal perfusion: comparison between two software-based algorithms for quantification. Surg Endosc 2021;35(09):5043–5050
41 van den Hoven P, Ooms S, van Manen L, et al. A systematic review of the use of near-infrared fluorescence imaging in patients with peripheral artery disease. J Vasc Surg 2019;70 (01):286–297.e1
42 Meijer RPJ, van Manen L, Hartgrink HH, et al. Quantitative dynamic near-infrared fluorescence imaging using indocyanine green for analysis of bowel perfusion after mesenteric resection. J Biomed Opt 2021;26(06):060501